Anisotropy of Domain Wall Resistance

M. Viret,[1] Y. Samson,[2] P. Warin,[1] A. Marty,[2] F. Ott,[1] E. Søndergård,[1] O. Klein,[1] and C. Fermon[1]

[1]*Service de Physique de l'Etat Condensé, Orme des Merisiers, CEA Saclay, 91191 Gif-sur-Yvette, France*
[2]*Laboratoire Nanostructure et Magnétisme, DRFMC/SP2M, CEA-Grenoble, 38054 Grenoble, France*

(Received 11 February 2000)

The resistive effect of domain walls in FePd films with perpendicular anisotropy was studied experimentally as a function of field and temperature. The films were grown directly on MgO substrates, which induces an unusual virgin magnetic configuration composed of 60 nm wide parallel stripe domains. This allowed us to carry out the first measurements of the anisotropy of domain wall resistivity in the two configurations of current perpendicular and parallel to the walls. At 18 K, we find 8.2% and 1.3% for the domain wall magnetoresistance normalized to the wall width (8 nm) in these two respective configurations. These values are consistent with the predictions of Levy and Zhang.

PACS numbers: 75.70.Kw, 72.15.Gd

Spin scattering in magnetically inhomogeneous regions has been the object of intense research in the past ten years. The discovery of giant magnetoresistance (GMR) and its potential applications have boosted studies of spin-dependent transport mainly in magnetic heterostructures [1] and granular materials [2] where the effect can be large. It is only recently that the scattering due to magnetic domain walls has been studied in the light of the theories developed for GMR [3–7]. Earlier studies include the work of Cabrera and Falicov [8] who used the WKB approximation to calculate the reflection coefficient of conduction electrons, thus estimating the resistance as a function of wall thickness which was found to be negligible in 3*d* ferromagnets. Berger [9] then described the wall crossing by electrons as "purely adiabatic" for their spin because the wall width is much greater than the Fermi wavelength, but mentioned a possible wiggling of the electron's trajectory because of Hall effect associated with the wall magnetization. More recent theoretical attempts to understand the transport across the domain wall based on the GMR effect started with the work of Viret *et al.* [3]. The authors considered that the electron spin starts to precess around the locally changing magnetization direction once the electron hits the domain wall. According to their calculations, the spin mistracking induces a resistance which favorably compares with experimental data on Co and Ni films [3]. Then, Levy and Zhang developed a quantum mechanical description based on the GMR Hamiltonian which leads to an increased resistance due to the mixing of the spin conduction channels induced by magnetization rotation within the domain wall. Noticeably, they were the first to derive both the CIW (current in wall) and CPW (current perpendicular to wall) resistances [4].

Experimentally, a positive domain wall resistivity has been measured in Co [3,6,9,10], Ni [3], and FePd [5]. None of these measurements have allowed one to extract the CPW and CIW effects. Surprisingly, Ruediger *et al.* [11] measured a domain wall induced decrease of resistance in epitaxial Fe structures. A negative contribution was indeed predicted by Tatara and Fukuyama [12] who considered the effect of a wall on the weak localization induced by impurity scattering. However, this quantum-mechanical correction should be relevant only at low temperature and not applicable to very pure Fe films at 65.5 K. Another possible origin for a decrease of the resistance induced by domain walls has been pointed out by van Gorkom *et al.* [7]. By taking into account the modifications of the band structure induced by the rotation of the magnetization within the wall, they showed that the resistance can be positive or negative as a function of the spin-dependent scattering lifetimes of the two (up and down) spin conduction channels.

A general problem in domain wall resistance measurements is to get rid of the anisotropic magnetoresistance (AMR). This effect originates in spin-orbit coupling and depends on the angle between the current lines and the local magnetization. In the case of a thin film where all the domains are in-plane, it is possible to circumvent the problem by careful angular measurements and by adding the resistance measured at 0° and 90° relative to the (in-plane) applied magnetic field [3]. The AMR contribution of in-plane magnetization domains disappears in this sum. However, the magnetization in the walls themselves often points out-of-plane and hence their AMR do not cancel out. In the general case of a crystal, the contribution of the AMR can be precisely taken into account only by carrying out measurements in the three directions of space (which has not yet been done). For thin films with out-of-plane anisotropy [5,10], the domains themselves do not contribute to vary the AMR since their magnetization is always perpendicular to the applied current. However, the exact configuration of the magnetization in the walls depends on the ratio of anisotropy to demagnetization energies: $Q = 2K/(\mu_0 M_s^2)$, with K the aniostropy energy and M_s the saturated bulk magnetization. For $Q < 1$, wall profiles can be rather complex [13] and the 3D resistivity tensor is required to properly account for the AMR of the walls themselves. Original measurements on *c*-axis oriented Co films ($Q = 0.4$) by Gregg *et al.* have shown a substantial effect which was analyzed in terms of domain

 0031-9007/00/85(18)/3962(4)$15.00

wall scattering [10]. However, recently Rüdiger *et al.* [14] remeasured similar Co films and analyzed the data taking into account the AMR contributions in the Néel caps of the walls. Their conclusion was that this AMR alone can account for the magnetoresistance, and any scattering contribution from the walls is very small and not consistent with the existing models. FePd alloys offer a more appropriate system because higher Q factors lead to a reduction of the Néel caps and hence reduce the AMR problem. Ravelosona *et al.* [5] carried out measurements on FePd films ($Q = 1.4$) where a clear contribution of domain wall scattering to the magnetoresistance could be demonstrated. Unfortunately, the isotropic domain configuration prevented the extraction of the CPW and CIW terms and a proper analysis of the wall AMR contribution was not carried out.

We present here results obtained on a FePd film with $Q = 1.5$ and with a domain configuration in parallel stripes enabling us to extract for the first time both the CIW and CPW wall resistivities. The 50 nm FePd film was grown in molecular beam epitaxy by coevaporation of Fe and Pd on a MgO(001) substrate held at 620 K. The absence of any seed layer allows a direct measurement of the FePd resistance. Furthermore, the growth process leads to a remanent state with a parallel stripe pattern as shown in the magnetic force microscopy (MFM) measurements of Fig. 1a. Remarkably, this ordered state results from the growth history [15] and is not recovered once the sample has been saturated by application of a perpendicular field (Fig. 1b). The period of the stripe pattern can be estimated at $2 \times d = 120$ nm in the virgin state and a quality factor $Q = 1.5$ is inferred from in-plane and out-of-plane hysteresis curves measured with a vibrating sample magnetometer. To determine the wall profile, we carried out numerical calculations using the 2D micromagnetic program OOMMF [16]. Taking the geometry of a semi-infinite, 50 nm thick 500 nm wide slab of FePd, the micromagnetic simulations reproduce almost exactly the period of the stripe pattern (120 nm) and provide the magnetization profile in the wall. This is shown in Fig. 2 where the relative importance of Bloch core and Néel caps are visible. The wall thickness can be defined as the width of the Bloch part which also corresponds roughly to the length on which the majority of the in-plane magnetization rotates in the Néel caps. It is found to be $\delta_w = 8$ nm.

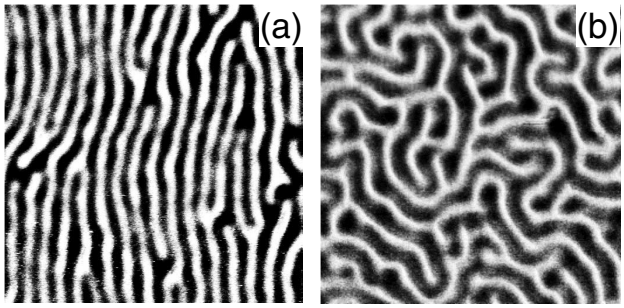

FIG. 1. 2×2 μm MFM images of (a) the virgin state where 60 nm wide domains lie in parallel stripes (b) the maze configuration obtained at zero field after magnetic saturation.

For the measurements, the films were patterned into a "Union Jack" geometry (see Fig. 3), so as to ensure an appropriate configuration for the current lines. For every measured point, the current was alternatively applied along the two main 100 μm wide stripes, i.e., parallel and perpendicular to the walls. Voltages were measured between the minor, diagonal stripes thus leading to the resistances and Hall effects in a four point geometry for both directions of the current lines. Figure 4 shows the normalized perpendicular magnetization extracted from the extraordinary Hall effect (EHE) data as a function of the out-of-plane applied field. On the figure, the measured remanence is almost zero and the only irreversible region is between the saturation and nucleation fields, respectively 0.85 T and 0.55 T. Figure 5 shows the corresponding longitudinal resistance measurements in the two current configurations (respectively, perpendicular and parallel to the walls) at 18 K. The resistances are maximum close to zero field where the domain wall density is the highest and minimum in the saturated state. The resistances can be expressed by

$$tR_\perp = \rho_s + \frac{\delta_w}{d}\rho_{\mathrm{cpw}} + \rho_{\mathrm{amr}\perp}$$

$$\text{and} \quad tR_\parallel = \rho_s + \frac{\delta_w}{d}\rho_{\mathrm{ciw}} + \rho_{\mathrm{amr}\parallel},$$

where t is the film thickness, $R_\perp$ and $R_\parallel$ the two measured resistances, ρ_s the resistivity in the (perpendicular) saturated state, ρ_{cpw} and ρ_{ciw} the extra CPW and CIW wall induced resistivities, $\rho_{\mathrm{amr}\perp}$ and $\rho_{\mathrm{amr}\parallel}$ the AMR contributions of in-plane magnetic moments, respectively perpendicular (Néel caps) and parallel to the walls, d the domain size, and δ_w the wall width. The expressions are valid in first order in $\frac{\delta_w}{d}\rho_{\mathrm{ciw}}$.

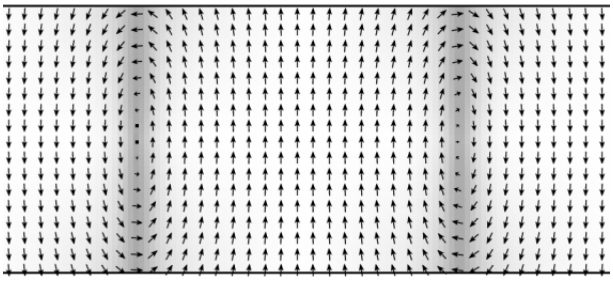

FIG. 2. Micromagnetic configuration in the cross section of a FePd slab taken infinite in the direction out of the page. The domain width is 60 nm and the wall is composed of 8 nm wide central Bloch sections with Néel caps of comparable length. The contributions to the total CPW and CIW resistances of the wall-induced AMR is found to be $\frac{\rho_{\mathrm{amr}\parallel}}{\rho_{\mathrm{amr}}} = 7.2\%$ and $\frac{\rho_{\mathrm{amr}\perp}}{\rho_{\mathrm{amr}}} = 3.8\%$.

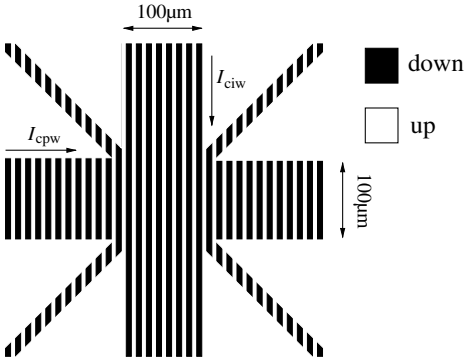

FIG. 3. Schematics of the measurement geometry: The "Union Jack" structure allows four point measurements parallel and perpendicular to the domain walls.

In Fig. 5, the two resistances (perpendicular and parallel to the walls) are almost exactly the same at saturation where a slight misalignment between the applied field and the film normal induces a small AMR difference. In the virgin state, the resistance measured with the current perpendicular to the walls is clearly larger than that parallel to the walls. In order to properly quantify ρ_{cpw} and ρ_{ciw}, we need to modify slightly the ideal picture leading to the expressions above. Indeed, two imperfect elements contribute to a mixing of the CPW and CIW geometries. First, the MFM pictures of Fig. 1 show that even in the prepared state, about 8% of domain walls are perpendicular to the direction of preferential alignment. Then, the current lines are not completely confined within the central square part of the cross and the current flowing out induces some mixing of $R_{\parallel}$ and $R_{\perp}$. According to a numerical estimation of the current lines using a conform transformation with a nondiagonal resistivity tensor, there is indeed a 12.5% mixing of the two resistances in our cross. Hence, considering a total of 21% mixing of the two geometries, and taking $d = 60$ nm, $\delta_w = 8$ nm, and $(\rho_{\mathrm{amr}\parallel} - \rho_{\mathrm{amr}\perp})/\rho_s = 1.5\%$ (which was inferred from resistivity measurements with the field in-plane), we find $\rho_{\mathrm{cpw}}/\rho_s = 8.2\%$ and $\rho_{\mathrm{ciw}}/\rho_s = 1.3\%$ within the walls. In the maze state, the average normalized wall resistivity is 4.5%, which is close to the middle of the two CPW and CIW resistivities. These results are in good agreement with the predictions of Levy and Zhang [4] for the two quantities as well as for the ratio $\frac{\rho_{\mathrm{cpw}}}{\rho_{ciw}} = 3 + \frac{10\sqrt{\rho_\uparrow \rho_\downarrow}}{\rho_\uparrow + \rho_\downarrow}$ which we measure at 6.3. Here $\rho_\uparrow$ and $\rho_\downarrow$ are the resistivities of the up and down conduction channels. This leads to a resistivity ratio $\rho_\uparrow/\rho_\downarrow \approx 10$. This result is consistent with band structure calculations which give an order of magnitude difference between up and down densities of states at the Fermi level [17].

Temperature measurements were also carried out and the variation of resistivity in the two configurations (CPW and CIW) was recorded. Figure 6 shows the difference $R_\perp - R_\parallel$ (which is roughly proportional to ρ_{cpw}), along with the average resistivity of the FePd alloy. We can observe that the wall resistivity does not follow the much steeper variation of the average resistivity. The former is approximately linearly decreasing with temperature while the latter is close to a variation in T^2. Presumably, the wall resistivity follows the variation of the density of polarized carriers with temperature while the bulk resistivity is the result of contributions from magnons, phonons, and impurity scattering. For pure Fe, the ratio of up to down densities of states at the Fermi level is known to vary appreciably with temperature. For FePd, however, the Fermi level lies well above the minority bands [17] and a temperature variation is not expected to affect this ratio noticeably. Arguably, the temperature variation of anisotropy in FePd could induce a slight change in the wall thickness, but there again, the effect should be small. Another quantity which could influence the DW scattering is the spin

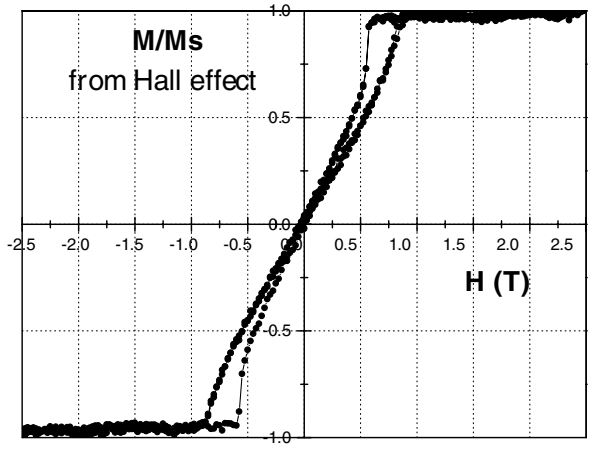

FIG. 4. Normalized magnetization loop extracted from the extraordinary Hall effect during perpendicularly applied field sweeps.

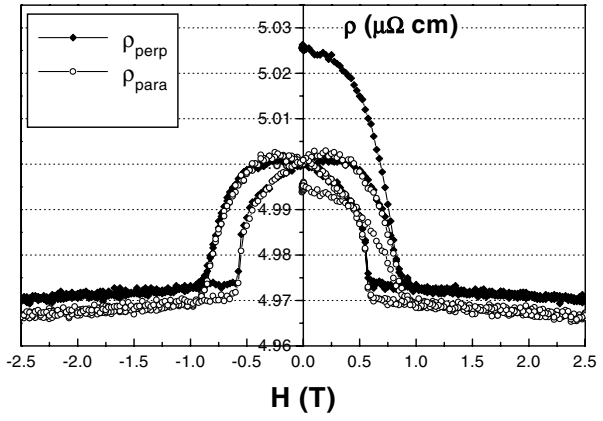

FIG. 5. Resistance variation along the two perpendicular directions during field sweeps. The excess resistances in the CPW and CIW configurations are, respectively, 1.1% and 0.50%. This reflects the asymmetric domain wall induced increase of resistivity.

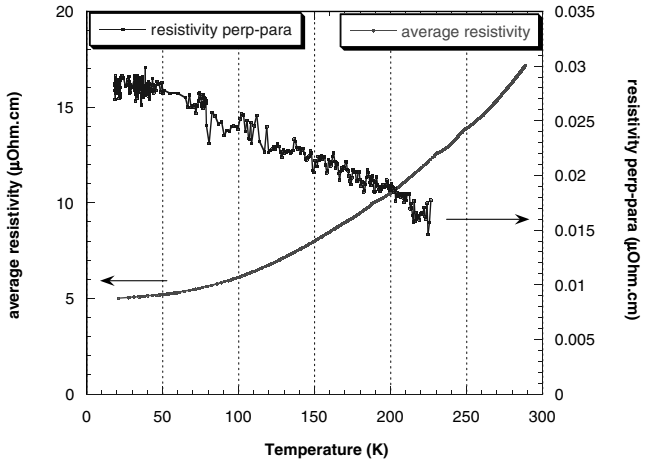

FIG. 6. Temperature dependence of the difference $R_\perp - R_\parallel$, which is roughly proportional to ρ_{cpw}, and the "bulk" resistivity.

mixing relaxation time $\tau_{\uparrow\downarrow}$. Its effect along with the variation of the ratio $\rho_\uparrow/\rho_\downarrow$ would reduce the DW resistivity with increasing temperature. In any case, a more quantitative analysis of the predicted domain wall resistance is needed to explain the temperature dependence of the CIW and CPW resistivities.

In conclusion, low-temperature measurements of the resistance induced by magnetic domain walls in FePd with perpendicular anisotropy in the CPW and CIW configurations have been carried out. Neither the negative contributions reported for Fe nor the large effects observed in head-to-head domain walls in Co [18] are present in this iron based alloy. FePd is an ideal system to test models of domain wall induced resistance because of the following reasons. First, the magnetization rotates at a similar pace in the Néel caps and the Bloch cores, hence the scattering should be approximately uniform within the wall. Also, in this high-Q material, the carriers experience a smooth change of magnetization while crossing slabs parallel to the wall. Hence, electronic transport could be well approximated by a one-dimensional problem where a charge (and spin) carrier enters an area of smoothly and uniformly varying local magnetization, which is the basic hypothesis of most models. The result is that a quantitative agreement is found with the model of Levy and Zhang [4]. This is the first time precise quantitative agreement is found with any of the published theories (with the possible exception of Ref. [3]). This provides strong support for the validity of this model.

We would like to thank A. Thiaville, D. Ravelosona, C. Chappert, C. Barreto, and J. C. Toussaint for fruitful discussions. We also acknowledge financial support from the European Union through the "Dynaspin" TMR network (FMR-X-CT97-0124).

[1] M. N. Baibich *et al.,* Phys. Rev. Lett. **61**, 2472 (1988).
[2] A. E. Berkowitz *et al.,* Phys. Rev. Lett. **68**, 3745 (1992).
[3] M. Viret *et al.,* Phys. Rev. B **53**, 8464 (1996).
[4] P. M. Levy and S. Zhang, Phys. Rev. Lett. **79**, 5110 (1997).
[5] D. Ravelosona *et al.,* Phys. Rev. B **59**, 4322 (1999).
[6] S. G. Kim *et al.,* IEEE Trans. Magn. **35**, 2862 (1999).
[7] R. P. van Gorkom, A. Brataas, and G. E. W. Bauer, Phys. Rev. Lett. **83**, 4401 (1999).
[8] G. G. Cabrera and L. M. Falicov, Phys. Stat. Solidi **61**, 539 (1974).
[9] L. Berger, J. Appl. Phys. **49**, 2156 (1978).
[10] J. Gregg *et al.,* Phys. Rev. Lett. **77**, 1580 (1996).
[11] U. Ruediger, J. Yu, S. Zhang, A. D. Kent, and S. S. P. Parkin, Phys. Rev. Lett. **80**, 5639 (1998).
[12] G. Tatara and H. Fukuyama, Phys. Rev. Lett. **78**, 3773 (1997).
[13] V. Gehanno, R. Hoffmann, Y. Samson, A. Marty, and S. Auffret, Eur. Phys. J. B **10**, 457 (1999).
[14] U. Rüdiger *et al.,* Phys. Rev. B **59**, 11 914 (1999).
[15] P. Kamp *et al.,* Phys. Rev. B **59**, 1105 (1999).
[16] Micromagnetic program in freeware on the NIST website.
[17] C. Barreto (private communication).
[18] P. Warin *et al.* (to be published).